

Spectrum and Energy Efficiency Evaluation of Two-Tier Femtocell Networks With Partially Open Channels

Xiaohu Ge, *Senior Member, IEEE*, Tao Han, *Member, IEEE*, Yan Zhang, *Senior Member, IEEE*, Guoqiang Mao, *Senior Member, IEEE*, Cheng-Xiang Wang, *Senior Member, IEEE*, Jing Zhang, *Member, IEEE*, Bin Yang, and Sheng Pan

Abstract—Two-tier femtocell networks are an efficient communication architecture that significantly improves throughput in indoor environments with low power consumption. Traditionally, a femtocell network is usually configured to be either completely open or completely closed in that its channels are either made available to all users or used by its own users only. This may limit network flexibility and performance. It is desirable for owners of femtocell base stations if a femtocell can partially open its channels for external-user access. In such scenarios, spectrum and energy efficiency becomes a critical issue in the design of femtocell network protocols and structure. In this paper, we conduct performance analysis for two-tier femtocell networks with partially open channels. In particular, we build a Markov chain to model the channel access in the femtocell network and then derive the performance metrics in terms of the blocking probabilities. Based on stationary state probabilities derived by Markov chain models,

spectrum and energy efficiency is modeled and analyzed under different scenarios characterized by critical parameters, including number of femtocells in a macrocell, average number of users, and number of open channels in a femtocell. Numerical and Monte Carlo (MC) simulation results indicate that the number of open channels in a femtocell has an adverse impact on the spectrum and energy efficiency of two-tier femtocell networks. Results in this paper provide guidelines for trading off spectrum and energy efficiency of two-tier femtocell networks by configuring different numbers of open channels in a femtocell.

Index Terms—Energy efficiency, femtocell networks, Markov chain, performance analysis, spectrum efficiency.

I. INTRODUCTION

TO accommodate the rapid increase in wireless data traffic in indoor environments, two-tier femtocell networks have been proposed to support the high spectrum efficiency in wireless communications [1], [2]. Particularly, energy efficiency in wireless communications has received much attention lately [3], [4]. It is important to study the spectrum and energy efficiency of femtocell networks for both economical and environmental considerations [5].

There are several studies on spectrum efficiency of femtocell networks in the literature [6]–[17]. They mainly focus on evaluating the impact of interference on the capacity and frequency reuse in wireless femtocell networks. Kim *et al.* derived the per-tier outage probability, i.e., the macrocell outage probability and the femtocell outage probability, by using a simplified mathematical model to closely approximate the femtocell interference distribution in a two-tier femtocell network [6]. Then, the capacity of the cochannel two-tier networks with outage probability constraints was obtained. Elkourdi and Simeone proposed a new approach to enable cooperation between femtocell and macrocell BSs [7]. In addition, the tradeoff between the outage probability and the diversity-multiplexing gains for both uplinks and downlinks was evaluated. Zhang focused on studying the blocking probability of femtocell networks assuming completely closed channel access. The paper recommended the use of a small number of split spectrum in a femtocell to increase the service availability in a macrocell [8]. In addition, Pantisano *et al.* [9] adopted a closed-access scheme at each femtocell to study the proposed novel framework of cooperation among femtocell and macrocell users. Results have shown that the performance of femtocell and macrocell users is limited

Manuscript received June 18, 2013; revised October 3, 2013; accepted November 11, 2013. Date of publication November 21, 2013; date of current version March 14, 2014. This work was supported in part by the National Natural Science Foundation of China (NSFC) under Grant 60872007 and Grant 61271224, by the NFSC Major International Joint Research Project under Grant 61210002, by the Ministry of Science and Technology of China under Grant 0903, by the Hubei Provincial Science and Technology Department under Grant 2011BFA004 and Grant 2013BHE005, by the Fundamental Research Funds for the Central Universities under Grant 2011QN020 and Grant 2013ZZGH009, by Research Councils UK through the UK–China Science Bridges Project: R&D on (B)4G Wireless Mobile Communications (EP/G042713/1), by the European Commission FP7 Project EVANS under Grant 2010-269323, by the Research Council of Norway through the SmartGrids ERA-Net project PRO-NET under Project 217006, by the EU FP7-PEOPLE-IRSES through project S2EuNet under Grant 247083 and through project WiNDOW under Grant 318992, and by the Key Laboratory of Cognitive Radio and Information Processing (Guilin University of Electronic Technology), Ministry of Education, China, under Grant 2013KF01. The work of G. Mao was supported by the Australian Research Council Discovery projects DP110100538 and DP120102030. The review of this paper was coordinated by Prof. H. H. Chen. (*Corresponding author: T. Han.*)

X. Ge, T. Han, J. Zhang, B. Yang, and S. Pan are with the Department of Electronics and Information Engineering, Huazhong University of Science and Technology, Wuhan 430074, China (e-mail: xhge@mail.hust.edu.cn; hantao@mail.hust.edu.cn; zhangjing@mail.hust.edu.cn; yangbin@mail.hust.edu.cn; pansheng@mail.hust.edu.cn).

Y. Zhang is with the Simula Research Laboratory, Fornebu 1364, Norway (e-mail: yanzhang@iee.org).

G. Mao is with the School of Computing and Communications, University of ICT Technology, Sydney, Ultimo, NSW 2007, Australia, and also with the National ICT Australia, Sydney, NSW 1466, Australia (e-mail: g.mao@iee.org).

C.-X. Wang is with the Joint Research Institute for Signal and Image Processing, School of Engineering and Physical Sciences, Heriot-Watt University, Edinburgh, EH14 4AS, U.K. (e-mail: cheng-xiang.wang@hw.ac.uk).

Color versions of one or more of the figures in this paper are available online at <http://ieeexplore.ieee.org>.

Digital Object Identifier 10.1109/TVT.2013.2292084

by interference and delay, respectively. Based on stochastic geometric techniques, the transmission success probability is derived for two cases of closed- and open-access schemes at the femtocell, respectively [10]. Xiang *et al.* applied the cognitive radio technology in femtocell networks and formulated the downlink spectrum sharing problem as a mixed-integer nonlinear programming problem [11]. A joint channel allocation and fast power control scheme was proposed to improve the spectrum efficiency of femtocell networks [12]. Chandrasekhar and Andrews analyzed the effect of channel uncertainty on two-tier femtocell networks. The transmit power level was determined to provide the desired signal-to-interference-plus-noise ratio (SINR) for the indoor cell-edge femtocell users [13]. On that basis, the beam weight was further optimized to maximize the output SINR of macrocell and femtocell users. Sun *et al.* proposed an intertier and intratier interference mitigation strategy and applied the strategy to a partial cochannel assignment problem [14]. In their proposed scheme, macrocell users are divided into femto-interfering and regular users, and then, an auction-based subcarrier-allocation algorithm was developed for mitigating intratier interference and improving the spectrum efficiency in femtocell networks. Chandrasekhar *et al.* developed a link quality protection algorithm for progressively reducing the SINR targets when a cellular user is unable to meet its SINR target in a two-tier femtocell network [15]. Jo *et al.* discovered that both the open- and closed-loop control schemes can effectively compensate for the uplink throughput degradation of the macrocell BS in a two-tier femtocell network [16]. Xia *et al.* evaluated both the completely open and completely closed femtocell access schemes using theoretical analysis and simulations for code-division multiple-access, time-division multiple-access, and orthogonal frequency-division multiple-access scenarios [17].

Considering the low-power advantage of femtocells, energy efficiency in femtocell networks has attracted attention in recent studies [18]–[26]. Particularly, Hou and Laurenson showed that the cellular and femtocell heterogeneous network architecture is able to provide a high quality of service and significantly reduce power consumption [18]. Khirallah *et al.* proposed an approach to estimate the total energy consumption in homogeneous and heterogeneous networks with femtocell deployments [19]. Han *et al.* proposed a power-allocation strategy to optimize both spectral and energy efficiency for large-scale femtocell deployment [20]. Zhang *et al.* reported various power control and radio resource management schemes for long-term evolution advanced (LTE-A) networks employing femtocells [21]. Their results demonstrated that the femtocell provides an energy-efficient solution for indoor coverage in LTE-A networks. Cao and Fan validated the energy efficiency improvement by simulating LTE femtocell networks with realistic system parameters [22]. Domenico *et al.* proposed two radio resource management schemes to enhance the energy efficiency of two-tier femtocell networks and improve both macrocell and femtocell throughput [23]. Apio *et al.* presented a switch-off algorithm to reduce the power consumption of some stations during low-traffic periods in two-tier femtocell networks [24]. Ku *et al.* explored the tradeoff between the spectrum efficiency and energy efficiency in wireless networks [25]. Hong *et al.*

evaluated the energy–spectrum efficiency tradeoff in virtual MIMO systems [26].

In this paper, we study both spectrum efficiency and energy efficiency in a two-tier femtocell network. Different from traditional studies where a femtocell is configured to be either completely open or completely closed, we allow a subset of channels to be open and the other channels to be closed in a femtocell. In particular, some femtocell channels are open for all users, and the rest of femtocell channels can only be used by the femtocell’s own customers. We call this *partially open channel arrangement*. It is shown that this partially open channel arrangement is able to significantly improve network flexibility and satisfy different requirements from femtocell owners. Moreover, this *partially open channel arrangement* is valuable for trading off the spectrum and energy efficiency of two-tier femtocell networks by changing the number of open channels in a femtocell. We also conduct performance analysis for two-tier femtocell networks with partially open channels based on Markov chain models. Such analysis is important to quantitatively characterize the spectrum and energy efficiency in a two-tier femtocell network. Specifically, the major contributions of this paper are as follows.

- 1) A Markov chain model is presented for two-tier femtocell networks with partially open channels. Furthermore, based on the stationary state probabilities of equilibrium equations in the Markov chain model, the closed-form blocking probability models of femtocell and macrocell users are derived and analyzed.
- 2) Spectrum and energy efficiency models are proposed for two-tier femtocell networks with partially open channels based on the Markov chain model. Analytical results of spectrum and energy efficiency models provide guidelines for trading off the spectrum and energy efficiency of two-tier femtocell networks by configuring different numbers of open channels in a femtocell.
- 3) Numerical and Monte Carlo (MC) simulation results are compared to validate the accuracy of the analysis. Moreover, simulation results demonstrate the tradeoff between spectrum efficiency and energy efficiency in two-tier femtocell networks with partially open channels.

The rest of this paper is organized as follows. Section II describes the system model of a two-tier femtocell network with partially open channels. In Section III, a Markov chain state transition diagram is proposed to model the dynamics of a femtocell. Based on the Markov chain model, spectrum efficiency and energy efficiency are investigated for femtocell networks with partially open channels in Section IV. Section V gives the numerical results of and discussions on spectrum and energy efficiency. Finally, Section VI concludes this paper.

II. TWO-TIER FEMTOCELL NETWORK SYSTEM MODEL

Fig. 1 shows the system model of a two-tier femtocell network. A macrocell network consists of multiple macrocells that share the same bandwidth. A macrocell covers a regular circular region A_M with radius R_M , and a macrocell BS is located in the center of the circle. The macrocell BS has N_M channels that are

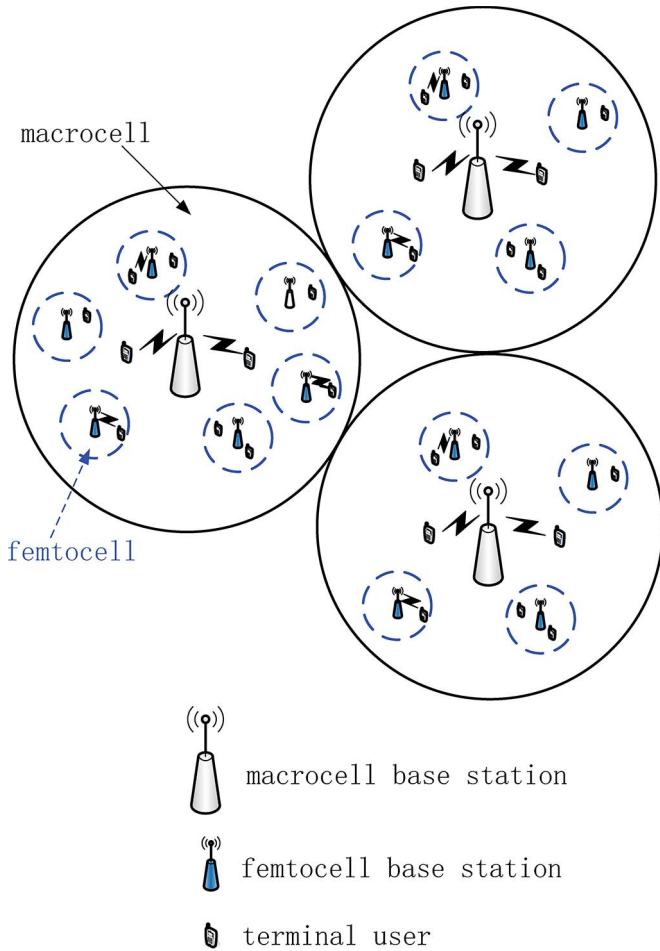


Fig. 1. Two-tier femtocell network system model.

open for all users. A femtocell covers a circular region A_F with radius R_F and a femtocell BS, which is usually called an access point, is located in the center of the femtocell. A femtocell BS has N_F channels that are classified into two types. One type of channel is open in the sense that it can be used by all users, whereas the other type of channel is called a closed channel, and it can only be used by femtocell users. The number of open femtocell channels is denoted by N_{F_O} , and the number of closed femtocell channels then becomes $N_F - N_{F_O}$ in a femtocell.

We consider two kinds of users in the two-tier femtocell networks: macrocell users and femtocell users. Macrocell users can access all unoccupied macrocell channels and unoccupied open femtocell channels when macrocell users are located in the corresponding coverage areas of these femtocells. Femtocell users can access all unoccupied macrocell channels and unoccupied femtocell channels in which these femtocell users are located. Within a specific femtocell, a femtocell user accesses the channels in the following order. A femtocell user will first access an unoccupied closed femtocell channel if there exists an unoccupied closed femtocell channel in the specific femtocell; a femtocell user will access an unoccupied open femtocell channel if all closed femtocell channels are busy and there exists an unoccupied open femtocell channel in the specific femtocell. Finally, the femtocell user will access an unoccupied macrocell

channel if all closed femtocell channels and open femtocell channels are busy in the specific femtocell. That is, a femtocell user can only access an unoccupied open femtocell channel when all closed femtocell channels are busy, and similarly for unoccupied macrocell channels. The macrocell network is overlaid with a femtocell network consisting of multiple femtocells. Femtocells do not overlap with each other. Therefore, users can hand off between a macrocell and a femtocell or between a macrocell and an adjacent macrocell. It is assumed that there are a total number of N femtocell BSs uniformly distributed within a macrocell, and furthermore, there are an average number of M femtocell users uniformly distributed in a femtocell. Without loss of generality, it is assumed that the traffic process originating from a user is governed by a Poisson process. Consequently, both the intertraffic arrival time and the traffic duration follow exponential distributions. To facilitate reading, the notations and symbols used in this paper are listed in Table I.

III. MARKOV CHAIN MODEL OF FEMTOCELL NETWORKS

Here, the number of occupied femtocell channels in a femtocell is first modeled by a Markov chain. By analyzing the Markov chain model, the blocking probabilities for a femtocell user and a macrocell user are derived, respectively. Furthermore, in the following section, the stationary state probabilities of the Markov chain model are derived to analyze the spectrum and energy efficiency of femtocell networks.

A. Markov Chain State Transition Model

To simplify the analysis using the Markov chain model, femtocells in a macrocell are considered a homogeneous system where all femtocells have the same equipment parameters. Furthermore, this homogeneous system is assumed to be in a statistical equilibrium, which means the average handoff arrival rate to a femtocell is equal to the corresponding handoff departure rate. This allows decoupling of a femtocell from its neighbors and permits an approximate analysis by consideration of the femtocell and its overlaying macrocell [27].

Let (i, j) denote the 2-D state of Markov chain modeling femtocell channel usage within a femtocell, where i represents the number of femtocell channels, including both open and closed femtocell channels, used by femtocell users, and j is the number of femtocell channels used by macrocell users in a femtocell. Fig. 2 shows the transition diagram of a femtocell. Now, we describe the state transitions in detail.

1) For $0 \leq i \leq N_F - N_{F_O}$ and $0 \leq j \leq N_{F_O}$, the following transitions may occur:

- $(i, j) \rightarrow (i + 1, j)$, when a closed femtocell channel is occupied by a new femtocell user call originating from a femtocell or handoff arrival to a femtocell, where $0 \leq i < N_F - N_{F_O}$.
- $(i, j) \rightarrow (i, j + 1)$, when an open femtocell channel is occupied by a new macrocell user call originating from a femtocell or handoff arrival to a femtocell, where $0 \leq j < N_{F_O}$.
- $(i, j) \rightarrow (i - 1, j)$, when a closed femtocell channel is released by a femtocell user call originating from a

TABLE I
NOTATIONS AND SYMBOLS USED IN THIS PAPER

Symbol	Definition/explanation
A_M, A_F	The areas of a macrocell and a femtocell, respectively
B_w	The bandwidth of femtocell channel
G	The standard random variable with a normal distribution
I_k	The interference power received from the k^{th} adjacent femtocell
L	The distance between the user and the corresponding femtocell BS
l	The distance between two femtocell BSs in a macrocell
M	The average number of femtocell users in a femtocell
N	The total number of femtocells within a macrocell
N_F, N_M	The number of channels in a femtocell and a macrocell, respectively
N_{F_O}	The number of open femtocell channels in a femtocell
n_0	The additive white Gaussian noise
n_w	The number of walls among femtocells in an indoor environment
P_{closed}, P_{open}	The occupancy probability of a closed femtocell channel and an open femtocell channel, respectively
P_{FU_F}, P_{MU_F}	The blocking probability of femtocell user and macrocell user in a femtocell, respectively
$P_{Handoff_MF}$	The hand-off probability from a macrocell to a femtocell
$P_{Handoff_FM}$	The hand-off probability from a femtocell to a macrocell
$P_{Handoff_MM}$	The hand-off probability from a macrocell to one of adjacent macrocells
P_{U_M}	The user blocking probability in a macrocell
PW_{FBS}	The total energy consumption of femtocell BS
PW_c, PW_t	The fixed and dynamic energy consumption of femtocell BS, respectively
PW_v	The transmission power over a femtocell channel
q	The fraction of femtocell calls to the total number of calls originating from a femtocell user
R_F, R_M	The radius of a femtocell and a macrocell, respectively
R_p	the protection distance between the user and the corresponding femtocell BS
S_m	The user desired signal power
T_{cF_F}, T_{cM_F}	The channel holding time of femtocell users and macrocell users in a femtocell, respectively
T_{cF_M}, T_{cM_M}	The channel holding time of femtocell user and macrocell user in a macrocell, respectively
T_F, T_M	The traffic intensity of femtocell users and macrocell users in a macrocell, respectively
$Z_{shadowing}$	The shadowing effect in an indoor environment
α^2	The random variable is exponentially distributed with mean value 1 in a Rayleigh fading environment
β	The path loss exponent over femtocell channels
η_{EE}	The utility function of energy efficiency
λ_1, λ_2	The aggregate traffic arrival rate of femtocell users and macrocell users in a femtocell, respectively
λ_T	The total traffic arrival rate in a macrocell and its underlying N femtocells
λ_F	The new traffic arrival rate of a femtocell user
$\lambda_{FU_F}, \lambda_{FU_M}$	The new traffic arrival rate of femtocell users originated from a femtocell and a macrocell, respectively
λ_{FU_FM}	The new arrival rate of femtocell users in macrocell which hand off from femtocells
$\lambda_{FU_H}, \lambda_{MU_H}$	The total handoff-in traffic arrival rate of femtocell users and macrocell users in a femtocell, respectively
λ_{FU_H}	The total handoff traffic arrival rate from a macrocell into a femtocell by all active femtocell users
λ_{FU_MM}	The handoff traffic arrival rate of all active femtocell users from an adjacent macrocell into the macrocell
λ_M	The total traffic arrival rate of all macrocell users
$\lambda_{MU_F}, \lambda_{MU_M}$	The new traffic arrival rate of macrocell users originated from a femtocell and a macrocell, respectively
λ_{MU_FM}	The new arrival rate of macrocell users in macrocell which hand off from femtocells
λ_{MU_H}	The total handoff traffic arrival rate from a femtocell into a macrocell by all active macrocell users
λ_{MU_MM}	The handoff traffic arrival rate of all active macrocell users from an adjacent macrocell into the macrocell
μ_1, μ_2	The rate of channel holding time of femtocell users and macrocell users in a femtocell, respectively
σ	The deviation parameter of log-normal shadowing
$1/\eta_{RT_F}, 1/\eta_{RT_M}$	The average dwelling time of femtocell users and macrocell users in a femtocell, respectively
$1/\mu$	The mean of user session duration

femtocell or handoff departure from a femtocell, where $0 < i \leq N_F - N_{F_O}$.

- $(i, j) \rightarrow (i, j - 1)$, when an open femtocell channel is released by a macrocell user call originating from a femtocell or handoff departure from a femtocell, where $0 < j \leq N_{F_O}$.

2) For $N_F - N_{F_O} \leq i \leq N_F$ and $0 \leq j \leq N_F - i$, the following transitions may occur:

- $(i, j) \rightarrow (i + 1, j)$, when an open femtocell channel is occupied by a new femtocell user call originating from a femtocell or handoff arrival to a femtocell. This event occurs when all closed femtocell channels are busy, where $N_F - N_{F_O} \leq i < N_F$.
- $(i, j) \rightarrow (i, j + 1)$, when an open femtocell channel is occupied by a new macrocell user call originating from a femtocell or handoff arrival to a femtocell, where $0 \leq j < N_F - i$.

- $(i, j) \rightarrow (i - 1, j)$, when an open femtocell channel is released by a femtocell user call originating from a femtocell or handoff departure from a femtocell. This event occurs when the femtocell user call has occupied an open femtocell channel, where $N_F - N_{F_O} < i \leq N_F$.
- $(i, j) \rightarrow (i, j - 1)$, when an open femtocell channel is released by a macrocell user call originating from a femtocell or handoff departure from a femtocell, where $0 < j \leq N_F - i$.

B. Analysis of the Markov Chain Model

In Fig. 1, we term a macrocell and its underlying N femtocells as an entity and assume that the total originating traffic process in an entity follows a Poisson process with arrive rate λ_T . For a femtocell user, it may generate both indoor, i.e., femtocell, and outdoor, i.e., macrocell, call activities although

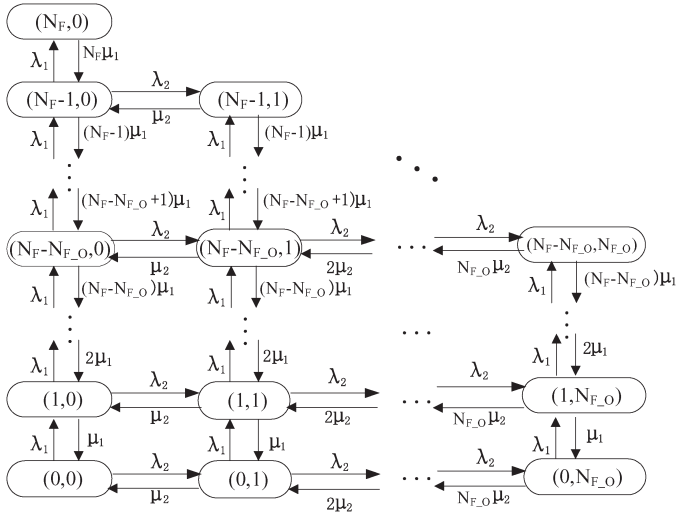


Fig. 2. State transition diagram in a femtocell.

indoor call activities occur more frequently. The fraction of indoor calls to the total number of calls originating from a femtocell user is denoted by q , and the new traffic arrival rate of a femtocell user is denoted by λ_F . Hence, the total traffic arrival rate of all macrocell users in an entity is $\lambda_M = \lambda_T - NM\lambda_F$. The total traffic arrival rate of all macrocell users in a femtocell is $(A_F/A_M) \cdot \lambda_M$, and the total traffic arrival rate of all macrocell users in a macrocell is $(1 - N(A_F/A_M))\lambda_M$. The user session duration, which refers to the time duration of a requested session connection, is assumed to be an exponential distribution with mean $1/\mu$. A user dwelling time refers to the time duration a user stays in a cell. The femtocell and macrocell users dwelling time in a femtocell is assumed to follow an exponential distribution with mean $1/\eta_{RT_F}$ and $1/\eta_{RT_M}$, respectively.

The aggregate traffic arrival rate of femtocell users λ_1 in a femtocell is divided into two parts. One part is the new traffic arrival rate of femtocell users λ_{FU_F} originating from a femtocell, and the other part is the total handoff in traffic arrival rate of femtocell users λ_{FU_H} caused by handoff from a macrocell into a femtocell by active femtocell users. Therefore, the aggregate traffic arrival rate of femtocell users λ_1 is determined by

$$\lambda_1 = \lambda_{FU_F} + \lambda_{FU_H}. \quad (1)$$

Moreover, the new traffic arrival rate of femtocell users λ_{FU_F} originating from a femtocell is given by

$$\lambda_{FU_F} = Mq\lambda_F. \quad (2)$$

Let P_{U_M} and P_{FU_F} denote the user-blocking probability in a macrocell and the blocking probability of femtocell users in a femtocell, respectively. Based on the results in (2) and Appendix A, the aggregate traffic arrival rate of femtocell users λ_1 is derived as follows:

$$\lambda_1 = Mq\lambda_F + \frac{1}{N}(\lambda_{FU_M} + \lambda_{FU_FM} + \lambda_{FU_MM}) \cdot (1 - P_{U_M}) \cdot P_{\text{Handoff_MF}} \quad (3a)$$

with

$$\lambda_{FU_M} = NM(1 - q) \cdot \lambda_F \quad (3b)$$

$$\lambda_{FU_FM} = N\lambda_1 \cdot (1 - P_{FU_F}) \cdot P_{\text{Handoff_FM}} \quad (3c)$$

$$\lambda_{FU_MM} = (\lambda_{FU_M} + \lambda_{FU_FM} + \lambda_{FU_MM}) \cdot (1 - P_{U_M}) \cdot P_{\text{Handoff_MM}}. \quad (3d)$$

The channel holding time of femtocell users T_{cF_F} with rate μ_1 in a femtocell is the minimum of the session duration and the average femtocell users dwelling time, i.e., $T_{cF_F} = \min(1/\mu, 1/\eta_{RT_F})$. Then, μ_1 is given by [28]

$$\mu_1 = \mu + \eta_{RT_F}. \quad (4)$$

The aggregate traffic arrival rate of macrocell users λ_2 in a femtocell is also divided into two parts. One part is the new traffic arrival rate of macrocell users λ_{MU_F} originating from femtocell itself, and the other part is the handoff in traffic arrival rate of macrocell users λ_{MU_H} caused by handoff from a macrocell into a femtocell by active macrocell users. Therefore, the aggregate traffic arrival rate of macrocell users λ_2 in a femtocell is calculated by

$$\lambda_2 = \lambda_{MU_F} + \lambda_{MU_H}. \quad (5)$$

Moreover, the new traffic arrival rate of macrocell users λ_{MU_F} is given by

$$\lambda_{MU_F} = \frac{A_F}{A_M} \lambda_M. \quad (6)$$

Let P_{MU_F} denote the blocking probability of a macrocell user in a femtocell. Based on the results in (6) and Appendix B, the aggregate traffic arrival rate of macrocell users λ_2 is derived as follows:

$$\lambda_2 = \frac{A_F}{A_M} \lambda_M + \frac{1}{N}(\lambda_{MU_M} + \lambda_{MU_FM} + \lambda_{MU_MM}) \cdot (1 - P_{U_M}) \cdot P_{\text{Handoff_MF}} \quad (7a)$$

with

$$\lambda_{MU_M} = \left(1 - N \frac{A_F}{A_M}\right) \cdot \lambda_M \quad (7b)$$

$$\lambda_{MU_FM} = N\lambda_2 \cdot (1 - P_{MU_F}) \cdot P_{\text{Handoff_FM}} \quad (7c)$$

$$\lambda_{MU_MM} = (\lambda_{MU_M} + \lambda_{MU_FM} + \lambda_{MU_MM}) \cdot (1 - P_{U_M}) \cdot P_{\text{Handoff_MM}}. \quad (7d)$$

The channel holding time of macrocell users T_{cM_F} with rate μ_2 in a femtocell is the minimum of the session duration and the average macrocell users dwelling time, i.e., $T_{cM_F} = \min(1/\mu, 1/\eta_{RT_F})$. Therefore, μ_2 is given by [28]

$$\mu_2 = \mu + \eta_{RT_M}. \quad (8)$$

Based on the Markov chain state transition diagram in Fig. 2, the set of equilibrium equations is given by (9), shown at the bottom of the next page, where $S(i, j)$ is the stationary state probability of Markov chain modeling femtocell channels in a

femtocell. After solving (9), a closed-form expression of state probability $S(i, j)$ is given by

$$S(i, j) = \frac{(\lambda_1/\mu_1)^i (\lambda_2/\mu_2)^j}{i!j!} S(0, 0). \quad (10)$$

The normalization condition is given by

$$\sum_{(i,j)} S(i, j) = 1. \quad (11)$$

From (11), the idle-state probability $S(0, 0)$, i.e., the probability that there is no active user using the channel, is derived as follows:

$$S(0, 0) = \left\{ \sum_{i=0}^{N_F} \sum_{j=0}^{\min(N_{F-O}, N_F-i)} \frac{(\lambda_1/\mu_1)^i (\lambda_2/\mu_2)^j}{i!j!} \right\}^{-1}. \quad (12)$$

As a consequence of the given equation, all other state probabilities can be obtained by substituting (12) into (10).

Note that the focus of this paper is on studying the call-blocking probability where an incoming call is blocked when there is no channel available in the network to serve the call. Based on the Markov chain state transition diagram in Fig. 2 and (10), the blocking probability of a femtocell user in a femtocell is given by

$$P_{FU-F} = \sum_{i=N_F-N_{F-O}}^{i=N_F} S(i, N_F - i). \quad (13)$$

Moreover, the blocking probability of a macrocell user in a femtocell is given by

$$P_{MU-F} = \sum_{i=0}^{i=N_F-N_{F-O}-1} S(i, N_{F-O}) + \sum_{i=N_F-N_{F-O}}^{i=N_F} S(i, N_F - i). \quad (14)$$

Based on the Erlang-B formula in [29], the user-blocking probability in a macrocell is given by

$$P_{U-M} = \frac{(T_M + T_F)^{N_M} / N_M!}{\sum_{k=0}^{N_M} (T_M + T_F)^k / k!} \quad (15)$$

where T_M and T_F are traffic intensities of macrocell and femtocell users in a macrocell, respectively. N_M is the number

of channels in a macrocell. Let T_{cM-M} denote the channel holding time of a macrocell user in a macrocell. It can be readily shown that the expectation of T_{cM-M} is given by [8]

$$E(T_{cM-M}) = \frac{1}{\mu + \eta_{RT-M}} \left[N \frac{A_F}{A_M} \cdot P_{MU-F} + \left(1 - N \frac{A_F}{A_M} \right) \right] + N \frac{A_F}{A_M} (1 - P_{MU-F}) \cdot E(Z) \quad (16a)$$

$$E(Z) = \frac{1}{\mu} - \frac{1}{\mu} \left[\frac{\ln\left(\frac{\mu}{\eta_{RT-M}}\right)}{\frac{\mu}{\eta_{RT-M}}} - \frac{\eta_{RT-M}}{\mu} \left(e^{-\frac{\eta_{RT-M}}{\mu}} - 1 \right) \right] \quad (16b)$$

where $E[\cdot]$ denotes an expectation operator. Then, the traffic intensity of macrocell users T_M in a macrocell is calculated by

$$T_M = (\lambda_{MU-M} + \lambda_{MU-FM} + \lambda_{MU-MM}) \cdot E(T_{cM-M}). \quad (17)$$

Let T_{cF-M} denote the channel holding time of a femtocell user in a macrocell. The expectation of T_{cF-M} is given by [8]

$$E(T_{cF-M}) = \frac{1}{\mu + \eta_{RT-M}} \left[N \frac{A_F}{A_M} \cdot P_{FU-F} + \left(1 - N \frac{A_F}{A_M} \right) \right] + N \frac{A_F}{A_M} (1 - P_{FU-F}) \cdot E(Z). \quad (18)$$

Furthermore, the traffic intensity of femtocell user T_F in a macrocell is given by

$$T_F = (\lambda_{FU-M} + \lambda_{FU-FM} + \lambda_{FU-MM}) \cdot E(T_{cF-M}). \quad (19)$$

Substituting (17) and (19) into (15), a closed-form user-blocking probability in a macrocell is derived. Equations (13)–(15) represent a nonlinear system, which can be solved by numerical techniques.

C. Analysis of Blocking Probabilities

Based on the proposed blocking probability models for two-tier femtocell networks, performance evaluation is analyzed as follows. Unless otherwise specified, the key parameters are configured as: $R_M = 1000$ m, $R_F = 20$ m, $N = 40$, $N_F = 3$, $N_{F-O} = 1$, $N_M = 24$, $q = 0.6$, $\lambda_F = 0.002$, and M is 4, 6, and 8 [30], [31]. The average value of the user session duration is set as $1/\mu = 110$ s [32]. The average values of femtocell and

$$\begin{cases} (\lambda_1 + \lambda_2 + \mu_1 i + \mu_2 j) S(i, j) = (i+1) \mu_1 S(i+1, j) \\ \quad + (j+1) \mu_2 S(i, j+1) + \lambda_1 S(i-1, j) + \lambda_2 S(i, j-1), & 0 \leq i \leq N_F, 0 \leq j \leq \min(N_{F-O}, N_F - i) \\ (\lambda_1 + \lambda_2 + \mu_1 i + \mu_2 j) S(i, j) = (i+1) \mu_1 S(i+1, j) \\ \quad + (j+1) \mu_2 S(i, j+1) + \lambda_2 S(i, j-1), & i = 0 \\ (\lambda_1 + \lambda_2 + \mu_1 i + \mu_2 j) S(i, j) = (i+1) \mu_1 S(i+1, j) \\ \quad + (j+1) \mu_2 S(i, j+1) + \lambda_1 S(i-1, j), & j = 0 \\ (\lambda_1 + \mu_1 i + \mu_2 N_{F-O}) S(i, j) = (i+1) \mu_1 S(i+1, j) \\ \quad + \lambda_1 S(i-1, j) + \lambda_2 S(i, j-1), & j = N_{F-O} \\ (\mu_1 i + \mu_2 (N_F - i)) S(i, j) = + \lambda_1 S(i-1, j) + \lambda_2 S(i, j-1), & i+j = N_F \end{cases} \quad (9)$$

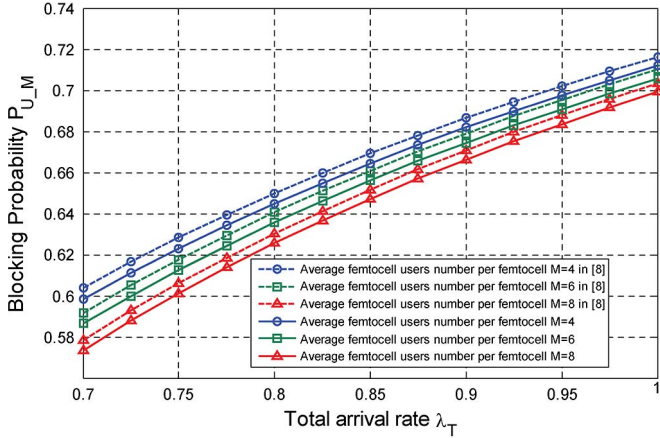


Fig. 3. User-blocking probability in terms of total arrival rate with different average numbers of femtocell users.

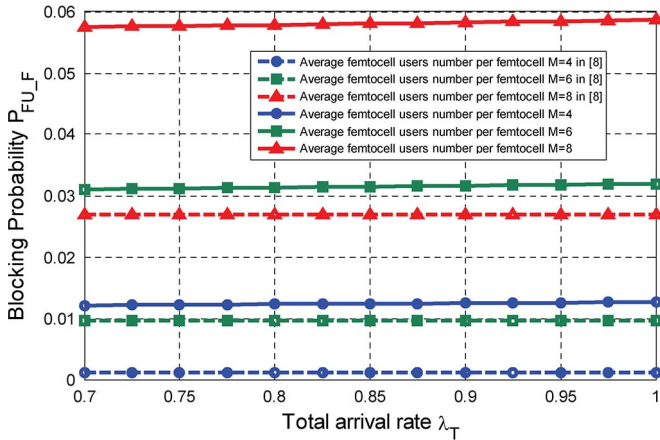


Fig. 4. Blocking probability of femtocell users in terms of total arrival rate with different average numbers of femtocell users.

macrocell users dwelling time in a femtocell are configured as $1/\eta_{RT-F} = 990$ and $1/\eta_{RT-M} = 300$ s [8], [11], respectively. To validate the proposed model, we compare the proposed model with the model derived in [8] in Figs. 3 and 4.

Fig. 3 shows the user-blocking probability $P_{U,M}$ in a macrocell in terms of the total arrival rate λ_T with different average numbers of femtocell users in a femtocell. The curves in Fig. 3 show that the value of $P_{U,M}$ increases with an increase in the arrival rate λ_T . When the number of occupied channels increases as a consequence of an increase in the arrival rate in a macrocell, the user-blocking probability in a macrocell $P_{U,M}$ increases. When the total arrival rate λ_T is fixed, it is interesting to see that the user-blocking probability $P_{U,M}$ decreases with an increase in the average number of femtocell users in a femtocell. This is caused by that an increase in the average number of femtocell users in a femtocell will reduce the traffic flow density in a macrocell when the total arrival rate λ_T is fixed. As a consequence, the user-blocking probability $P_{U,M}$ decreases when more users are added into a femtocell. The curves obtained from the proposed model exhibit a good match with the curves obtained from the model in [8]. This result indicates that the proposed model is consistent with the model in [8] if the impact of closed and open femtocell channels is not considered in simulation results.

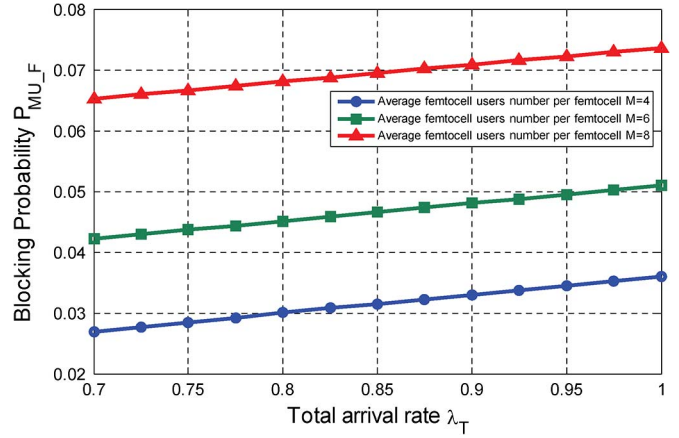


Fig. 5. Blocking probability of macrocell users in terms of total arrival rate with different average numbers of femtocell users.

Fig. 4 shows the blocking probability of femtocell users $P_{F,U,M}$ in terms of the total arrival rate λ_T with different average numbers of femtocell users in a femtocell. The curves in Fig. 4 show that the blocking probability of femtocell users $P_{F,U,M}$ increases with the higher total arrival rate λ_T . We can also observe that when the total arrival rate λ_T is fixed, the blocking probabilities of femtocell users increase with an increase in the average number of femtocell users. Compared with the curves obtained from the model in [8], the curves obtained from the proposed model demonstrate the same trend in Fig. 4. In the proposed model, femtocell channels are not only open for femtocell users but also partially open to macrocell users. In the model derived in [8], femtocell channels are only open for femtocell users. In this case, the blocking probability derived from the proposed model is higher than the blocking probability in [8].

Fig. 5 analyzes the blocking probability of macrocell users $P_{M,U,M}$ in terms of the total arrival rate λ_T with different average numbers of femtocell users in a femtocell. Numerical results show that the blocking probability of macrocell users $P_{M,U,M}$ increases with the higher total arrival rate λ_T . Moreover, when the total arrival rate λ_T is fixed, the blocking probability of macrocell users increases with an increase in the average number of femtocell users in a femtocell.

IV. SPECTRUM AND ENERGY EFFICIENCY MODELS OF FEMTOCELL NETWORKS

Based on the stationary state probabilities derived by the Markov chain models, the spectrum and energy efficiency models are proposed for femtocell networks. Furthermore, simulations are performed to analyze the performance parameters of spectrum and energy efficiency in femtocell networks.

A. Spectrum Efficiency Model of Femtocell Networks

The occupancy probability of a closed femtocell channel is analyzed by considering two situations separately. In the first situation, the number of channels occupied by femtocell users is smaller than or equal to the number of closed femtocell channels in a femtocell; in the second situation, the number of

channels occupied by femtocell users is larger than the number of closed femtocell channels in a femtocell. Therefore, using (10), the occupancy probability of a closed femtocell channel is given by

$$P_{\text{closed}} = \sum_{i=1}^{N_F - N_{F_O}} \sum_{j=0}^{N_{F_O}} \frac{\binom{N_F - N_{F_O} - 1}{i-1}}{\binom{N_F - N_{F_O}}{i}} S(i, j) + \sum_{i=N_F - N_{F_O} + 1}^{N_F} \sum_{j=0}^{N_F - i} S(i, j) \quad (20)$$

where $\binom{x}{y}$ is the binomial coefficients with parameters x and y . Similarly, the occupancy probability of an open femtocell channel can also be analyzed by considering two situations separately. The first situation occurs when the femtocell users do not occupy the open femtocell channels in a femtocell. The second situation occurs when the femtocell users occupy the open femtocell channels in a femtocell. Therefore, using (10), the occupancy probability of an open femtocell channel is given by

$$P_{\text{open}} = \sum_{i=0}^{N_F - N_{F_O}} \sum_{j=1}^{N_{F_O}} \frac{\binom{N_{F_O} - 1}{j-1}}{\binom{N_{F_O}}{j}} S(i, j) + \sum_{i=N_F - N_{F_O} + 1}^{N_F} \sum_{j=0}^{N_F - i} \frac{\binom{N_{F_O} - 1}{i - (N_F - N_{F_O}) - 1}}{\binom{N_{F_O}}{i - (N_F - N_{F_O})}} S(i, j). \quad (21)$$

Considering that femtocells are assumed to be uniformly distributed in a macrocell, the probability density function (pdf) of distance l between two femtocell BSs in a macrocell is given by [33]

$$f(l) = \frac{4l}{\pi R_M^2} \left(\arccos \left(\frac{l}{2R_M} \right) - \frac{l}{2R_M} \sqrt{1 - \left(\frac{l}{2R_M} \right)^2} \right) \quad (22)$$

where $0 \leq l \leq 2R_M$. Moreover, considering that the distance between a user and its associated femtocell BS is usually small, the distance between a user and the interfering femtocell BS is approximated by the distance between the associated femtocell BS and the interfering femtocell BS.

To avoid cochannel interference between macrocells and femtocells, it is assumed that macrocells and femtocells use different frequencies for communications. Furthermore, all femtocells in a macrocell share the same frequency bandwidth, and the frequency bandwidth used by a femtocell is divided into N_F no-overlapping subbandwidth. Here, each frequency subbandwidth corresponds to a femtocell channel. In this case,

the number of interfering users from adjacent femtocells is no more than the number of femtocells in a macrocell. For the sake of illustration, the number of interfering users from an adjacent femtocell is configured as one. Since the radius of a macrocell is much larger than the radius of a femtocell, the cochannel interference from adjacent macrocells is ignored in this paper. Furthermore, a user in a femtocell is only interfered by users using the same frequency subbandwidth in adjacent femtocells and located in the same macrocell. We consider the propagation effects of path loss, shadowing, and Rayleigh fading over femtocell channels. When an active user is located in a femtocell, the active user receives interference from the k th adjacent femtocell, i.e., $1 \leq k \leq N - 1$. The interference power originating from the k th adjacent femtocell is expressed as [34]–[36]

$$I_k = PW_v \frac{e^{2\sigma G} \alpha^2}{10^{1.2n_w} l^\beta} \quad (23)$$

where PW_v is the transmission power over a femtocell channel. The total transmission power of a femtocell is distributed over all femtocell channels. The term $e^{2\sigma G}$ accounts for lognormal shadowing with deviation σ , where $G \sim \text{Gaussian}(0, 1)$ represents a standard normal random variable. The random variable α^2 is exponentially distributed with mean value 1 in a Rayleigh fading environment. The item $10^{1.2n_w}$ refers to the through-wall loss in an indoor environment with the number of walls among femtocells n_w . The item l^β stands for the path loss effect between two femtocells within a macrocell with path loss exponent β .

Considering that femtocells are usually used for indoor environment, the signal received by a user in a femtocell does not consider the small-scale fading and the through-wall loss. Therefore, the desired signal power S_m received by the m th user in a femtocell is given by

$$S_m = PW_v \frac{Z_{\text{shadowing}}}{L^\beta} \quad (24)$$

where $Z_{\text{shadowing}}$ indicates the shadowing effect in an indoor environment and is assumed to be 4 dB [37]. L denotes the distance between user UE_m and the corresponding femtocell BS. Users are uniformly distributed in a femtocell, and the protection distance between the user and the corresponding femtocell BS is R_p . The pdf of L is given by

$$f(L) = \frac{2L}{R_F^2} \quad (25)$$

where $R_p \leq L \leq R_F$.

Furthermore, the capacity of all closed channels in a femtocell is derived by (26), shown at the bottom of the page,

$$C_{\text{closed}} = \sum_{m=1}^{N_F - N_{F_O}} B_W \log \left(1 + \frac{P_{\text{closed}} S_m}{n_0 + \sum_{n=1}^{N-1} \binom{N-1}{n} \left(\frac{P_{\text{closed}}}{N_F - N_{F_O}} \right)^n \left(1 - \frac{P_{\text{closed}}}{N_F - N_{F_O}} \right)^{N-1-n} \sum_{k=1}^n I_k} \right) \quad (26)$$

where n_0 denotes the additive white Gaussian noise in wireless channels. B_W represents the bandwidth of a femtocell channel. The capacity of all open channels in a femtocell is derived by (27), shown at the bottom of the page. As a consequence, the total capacity of a femtocell is derived by (28), shown at the bottom of the page.

B. Energy Efficiency Model of Femtocell Networks

Femtocell BS energy consumption can be decomposed into the fixed-energy-consumption part and the dynamic-energy-consumption part [3]. Fixed energy consumption, e.g., circuit energy consumption, is the baseline energy consumed at a femtocell BS. Circuit energy consumption usually depends on both the hardware and software configurations of a femtocell BS and is independent of the number of occupied channels. Dynamic energy consumption accounts for the transmission energy consumed in radio frequency transmission circuits depending on the number of occupied channels. As an easy consequence of the given analysis, we can build a femtocell BS energy consumption model, i.e.,

$$E(PW_{FBS}) = PW_c + E(PW_t) \quad (29)$$

where PW_{FBS} denotes the total energy consumption of a femtocell BS. PW_c refers to the fixed energy consumption of a femtocell BS. PW_t indicates the dynamic energy consumption of a femtocell BS. The dynamic energy consumption is mainly associated with the transmission energy over wireless channels. Based on the Markov chain state transition diagram in Fig. 2, the average dynamic energy consumption is derived as follows:

$$E(PW_t) = \sum_{i=0}^{N_F} \min(N_{F-O}, N_{F-i}) \sum_{j=0}^{N_F-i} (i+j) S(i, j) PW_v. \quad (30)$$

It is very important to study the spectrum and energy efficiency from a systematic perspective. For this, we introduce a new performance metric called the *utility function of energy efficiency*, which is defined as the ratio of the total capacity in a femtocell to the average total energy consumption in a femtocell BS. Let η_{EE} denote the utility function of energy efficiency. Then, we have

$$\eta_{EE} = \frac{E(PW_{FBS})}{C_{\text{total}}}. \quad (31)$$

Based on (28) and (29), the energy efficiency model can be further derived as in (32a) and (32b), shown at the bottom of the next page.

V. NUMERICAL RESULTS AND DISCUSSIONS

Here, numerical and MC simulations are presented to demonstrate interactions between the femtocell energy efficiency metrics and critical performance-impacting parameters. Unless otherwise specified, the following parameters are used in the numerical and MC simulations: $\sigma = 8$ dB, $\beta = 2$, $n_w = 2$, and $R_p = 5$ m.

First, we fix the number of total femtocell channels $N_F = 6$ and the number of open femtocell channels $N_{F-O} = 3$. Fig. 6 shows the spectrum efficiency of the femtocell networks in terms of the average number of femtocell users with different numbers of femtocells in a macrocell, in which “Num” labels the numerical results, and “MC” represents the MC simulation results. When the number of femtocells in a macrocell is fixed, the spectrum efficiency increases with an increase in the average number of users in a femtocell. When the average number of users in a femtocell is fixed, the spectrum efficiency of femtocell networks decreases with an increase in the number of femtocells in a macrocell. Fig. 7 shows the energy efficiency of the femtocell networks in terms of the average

$$C_{\text{open}} = \sum_{m=1}^{N_{F-O}} B_W \log \left(1 + \frac{P_{\text{open}} S_m}{n_0 + \sum_{n=1}^{N-1} \binom{N-1}{n} \left(\frac{P_{\text{open}}}{N_{F-O}} \right)^n \left(1 - \frac{P_{\text{open}}}{N_{F-O}} \right)^{N-1-n} \sum_{k=1}^n I_k} \right) \quad (27)$$

$$C_{\text{total}} = C_{\text{closed}} + C_{\text{open}} = \sum_{m=1}^{N_F - N_{F-O}} B_W \log \left(1 + \frac{P_{\text{closed}} S_m}{n_0 + \sum_{n=1}^{N-1} \binom{N-1}{n} \left(\frac{P_{\text{closed}}}{N_F - N_{F-O}} \right)^n \left(1 - \frac{P_{\text{closed}}}{N_F - N_{F-O}} \right)^{N-1-n} \sum_{k=1}^n I_k} \right) + \sum_{m=1}^{N_{F-O}} B_W \log \left(1 + \frac{P_{\text{open}} S_m}{n_0 + \sum_{n=1}^{N-1} \binom{N-1}{n} \left(\frac{P_{\text{open}}}{N_{F-O}} \right)^n \left(1 - \frac{P_{\text{open}}}{N_{F-O}} \right)^{N-1-n} \sum_{k=1}^n I_k} \right) \quad (28)$$

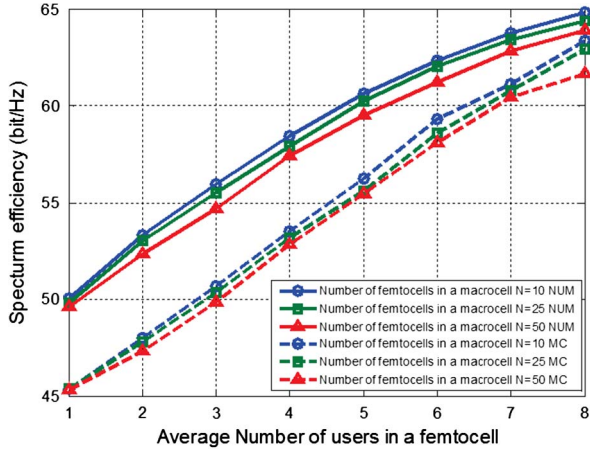


Fig. 6. Spectrum efficiency of femtocell networks with respect to the average number of users in a femtocell.

number of femtocell users with different numbers of femtocells in a macrocell. When the number of femtocells in a macrocell is fixed, the energy efficiency of femtocell networks increases with an increase in the average number of users in a femtocell. When the average number of users in a femtocell is fixed, the energy efficiency of femtocell networks increases with an increase in the number of femtocells in a macrocell. Compared with results from MC simulations, these numerical results are validated in Figs. 6 and 7, which demonstrate good accuracy of the results.

Second, we fix the number of open femtocell channels $N_{F_O} = 3$ and the average number of users as 4 in a femtocell. Fig. 8 shows the spectrum efficiency in terms of the number of closed channels in a femtocell with different numbers of femtocells in a macrocell. It is observed that the spectrum efficiency increases with an increase in the number of closed channels in a femtocell. In addition, when the number of closed channels is fixed, the spectrum efficiency of the femtocell networks decreases with an increase in the number of femtocells in a macrocell. Fig. 9 shows the energy efficiency performance in terms of the number of closed channels in a femtocell. We can observe that the energy efficiency of the femtocell networks

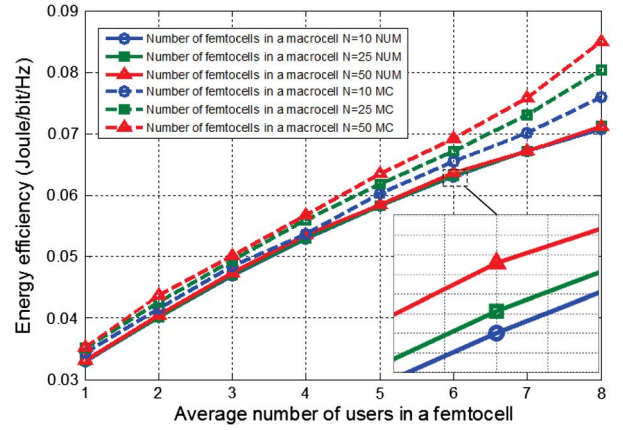


Fig. 7. Energy efficiency of femtocell networks with respect to the average number of users in a femtocell.

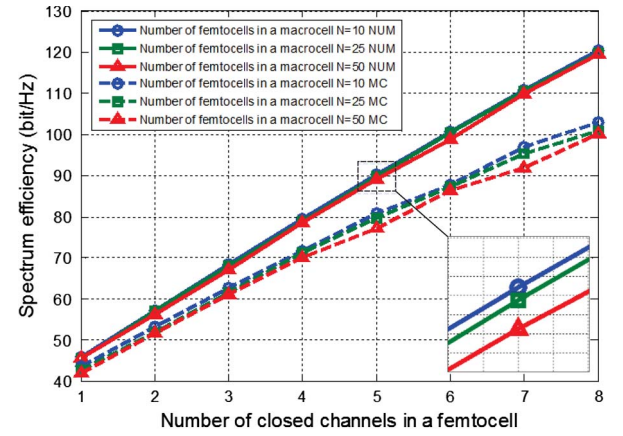


Fig. 8. Spectrum efficiency of femtocell networks with respect to the number of closed channels in a femtocell.

decreases with an increase in the number of closed channels in a femtocell. On the other hand, the energy efficiency increases with an increase in the number of femtocells in a macrocell. The numerical results are validated by the MC simulation results shown in Figs. 8 and 9. However, the MC simulation curves are less than the numerical curves in Figs. 8 and 9.

$$\eta_{EE} = \frac{PW_c + \sum_{i=0}^{N_F} \sum_{j=0}^{\min(N_{F_O}, N_F - i)} (i+j)S(i,j)}{C_{total}} (i+j)S(i,j)PW_v \quad (32a)$$

$$C_{total} = \sum_{m=1}^{N_F - N_{F_O}} B_W \log \left(1 + \frac{P_{closed} S_m}{n_0 + \sum_{n=1}^{N-1} \binom{N-1}{n} \left(\frac{P_{closed}}{N_F - N_{F_O}} \right)^n \left(1 - \frac{P_{closed}}{N_F - N_{F_O}} \right)^{N-1-n} \sum_{k=1}^n I_k} \right) + \sum_{m=1}^{N_{F_O}} B_W \log \left(1 + \frac{P_{open} S_m}{n_0 + \sum_{n=1}^{N-1} \binom{N-1}{n} \left(\frac{P_{open}}{N_{F_O}} \right)^n \left(1 - \frac{P_{open}}{N_{F_O}} \right)^{N-1-n} \sum_{k=1}^n I_k} \right) \quad (32b)$$

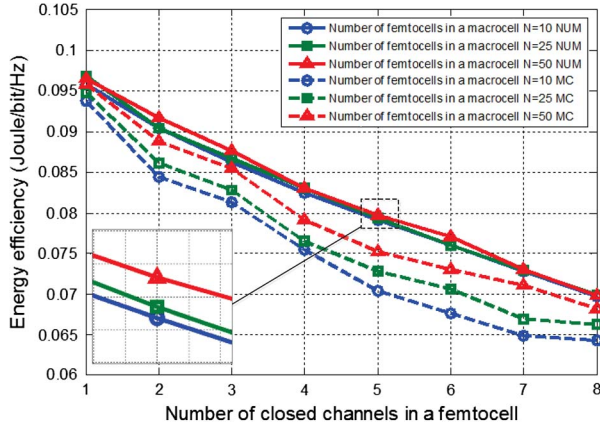


Fig. 9. Energy efficiency of femtocell networks with respect to the number of closed channels in a femtocell.

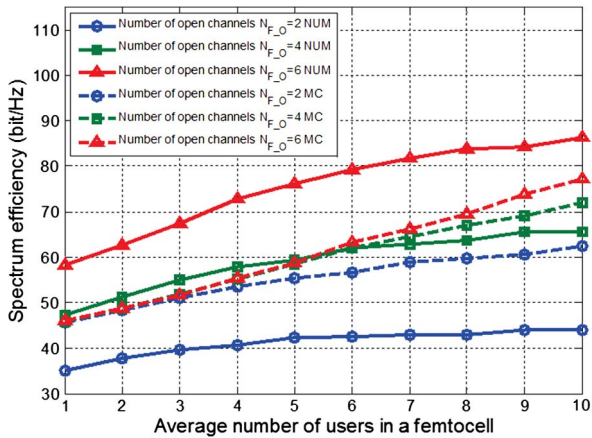


Fig. 10. Spectrum efficiency of femtocell networks with respect to the number of open channels.

Considering that the MC simulation results are realized by finite simulation calculations, a few MC simulation calculation values with small probabilities will be discarded in the final results.

In the end, we fix the number of closed femtocell channels to be 2 and the number of femtocells in a macrocell to be 25 for the following simulation. Fig. 10 shows the spectrum efficiency of the femtocell networks in terms of the average number of femtocell users with different numbers of open channels in a femtocell. In this example, the number of total channels in a femtocell is set as 8. We can see that the spectrum efficiency of the femtocell networks increases with an increase in the average number of users in a femtocell. When the average number of users is fixed in a femtocell, the spectrum efficiency increases with an increase in the number of open channels in a femtocell. Fig. 11 shows the energy efficiency of the femtocell networks in terms of the average number of femtocell users with different open channels in a femtocell. The curves show that the energy efficiency increases with an increase in the average number of users in a femtocell and that the energy efficiency decreases with an increase in the number of open channels in a femtocell. According to the energy efficiency model in (32), the average dynamic energy consumption linearly increases with an increase in the number of open femtocell channels; however,

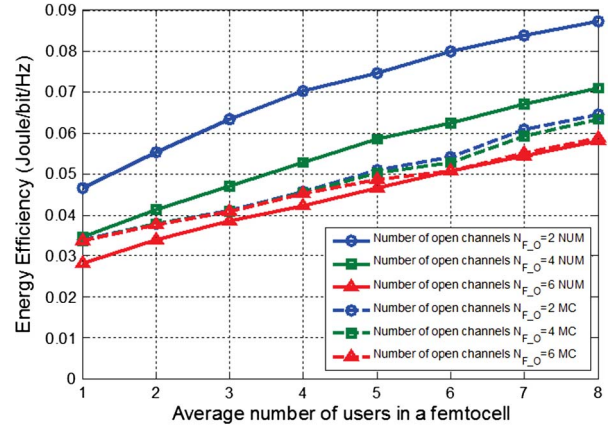


Fig. 11. Energy efficiency of femtocell networks with respect to the number of open channels.

the total capacity of a femtocell only increases logarithmically with an increase in the number of open femtocell channels. Therefore, when the number of open femtocell channels increases, the energy efficiency decreases. Based on the results in Figs. 8–11, our analytical models and simulation results indicate that an increase in the number of open or closed femtocell channels can conduce to the increase in spectrum efficiency and the decrease in energy efficiency in a two-tier femtocell network. As a consequence, the results provide useful guidelines for trading off the spectrum and energy efficiency of two-tier femtocell networks by configuring different numbers of open or closed femtocell channels in a femtocell.

VI. CONCLUSION

In this paper, the channel occupancy in a femtocell was modeled by Markov chains. To derive state transition probabilities in a femtocell, a Markov chain state transition diagram for a femtocell was presented. Moreover, the user-blocking probability in a macrocell and the blocking probabilities of femtocell and macrocell users in a femtocell were derived and analyzed. Furthermore, spectrum and energy efficiency models were proposed for two-tier femtocell networks with partially open channels. Simulation results have shown the impacts of critical parameters on the two-tier femtocell networks, including the number of femtocell users, the number of femtocells in a macrocell, and the number of open or closed channels in a femtocell. Our analysis indicates that the spectrum and energy efficiency of two-tier femtocell networks can be traded off by configuring different numbers of open channels in a femtocell. Moreover, the results of energy efficiency for two-tier femtocell networks can provide useful guidelines in determining the number of femtocells to deploy in a macrocell.

APPENDIX A

The handoff probability from a femtocell into a macrocell is defined as $P_{\text{Handoff}_{FM}}$, which is given by [8]

$$P_{\text{Handoff}_{FM}} = \frac{\eta_{RT_F}}{\mu + \eta_{RT_F}}. \quad (33)$$

The handoff probability from a macrocell into a femtocell is defined as $P_{\text{Handoff}_{MF}}$, which is given by [8]

$$P_{\text{Handoff}_{MF}} = \frac{A_F}{A_M} \cdot \left[\frac{\ln\left(\frac{\mu}{\eta_{RT_M}}\right)}{\frac{\mu}{\eta_{RT_M}}} - \frac{\eta_{RT_M}}{\mu} \left(e^{-\frac{\eta_{RT_M}}{\mu}} - 1 \right) \right]. \quad (34)$$

The handoff probability from a macrocell into one of the adjacent macrocells is defined as $P_{\text{Handoff}_{MM}}$, which is given by [8]

$$P_{\text{Handoff}_{MM}} = \frac{\eta_{RT_M}}{\mu + \eta_{RT_M}}. \quad (35)$$

Active femtocell users in a macrocell can be further divided into three types of femtocell users: 1) a femtocell user with a new call in the specified macrocell, whose traffic arrival rate is λ_{FU_M} ; 2) an active femtocell user handed off from a femtocell into the specified macrocell, whose traffic arrival rate is λ_{FU_FM} ; and 3) an active femtocell user handed off from an adjacent macrocell into the specified macrocell, whose traffic arrival rate is λ_{FU_MM} . In this case, λ_{FU_M} is expressed as

$$\lambda_{FU_M} = NM(1 - q) \cdot \lambda_F. \quad (36)$$

λ_{FU_FM} is given by

$$\lambda_{FU_FM} = N\lambda_1 \cdot (1 - P_{FU_F}) \cdot P_{\text{Handoff}_{FM}}. \quad (37)$$

To keep a balance in a stationary system, the outgoing traffic rate of femtocell users should be equal to the entering traffic rate of femtocell users in a macrocell [38]. Therefore, λ_{FU_MM} is given by

$$\lambda_{FU_MM} = (\lambda_{FU_M} + \lambda_{FU_FM} + \lambda_{FU_MM}) \cdot (1 - P_{U_M}) \cdot P_{\text{Handoff}_{MM}}. \quad (38)$$

Furthermore, the handoff in traffic arrival rate λ_{FU_H} is derived as

$$\lambda_{FU_H} = \frac{1}{N} (\lambda_{FU_M} + \lambda_{FU_FM} + \lambda_{FU_MM}) \cdot (1 - P_{U_M}) \cdot P_{\text{Handoff}_{MF}} \quad (39a)$$

$$\lambda_{FU_M} = NM(1 - q) \cdot \lambda_F \quad (39b)$$

$$\lambda_{FU_FM} = N\lambda_1 \cdot (1 - P_{FU_F}) \cdot P_{\text{Handoff}_{FM}} \quad (39c)$$

$$\lambda_{FU_MM} = (\lambda_{FU_M} + \lambda_{FU_FM} + \lambda_{FU_MM}) \cdot (1 - P_{U_M}) \cdot P_{\text{Handoff}_{MM}}. \quad (39d)$$

APPENDIX B

Active macrocell users in a macrocell can be further divided into three types of macrocell users: 1) a macrocell user with a new call in the specified macrocell, whose traffic arrival rate is λ_{MU_M} ; 2) an active macrocell user handed off from a femtocell into the specified macrocell, whose traffic arrival rate is λ_{MU_FM} ; and 3) an active macrocell user handed off from

an adjacent macrocell into the specified macrocell, whose traffic arrival rate is λ_{MU_MM} . In this case, λ_{MU_M} is given by

$$\lambda_{MU_M} = \left(1 - N \frac{A_F}{A_M} \right) \cdot \lambda_M. \quad (40)$$

λ_{MU_FM} is given by

$$\lambda_{MU_FM} = N\lambda_2 \cdot (1 - P_{MU_F}) \cdot P_{\text{Handoff}_{FM}}. \quad (41)$$

To keep a balance in a stationary system, the leaving traffic rate of macrocell users should be equal to the entering traffic rate of macrocell users in a macrocell [38]. Therefore, λ_{MU_MM} is given by

$$\lambda_{MU_MM} = (\lambda_{MU_M} + \lambda_{MU_FM} + \lambda_{MU_MM}) \cdot (1 - P_{U_M}) \cdot P_{\text{Handoff}_{MM}}. \quad (42)$$

Furthermore, the handoff traffic arrival rate of macrocell users λ_{MU_H} is derived by

$$\lambda_{MU_H} = \frac{1}{N} (\lambda_{MU_M} + \lambda_{MU_FM} + \lambda_{MU_MM}) \cdot (1 - P_{U_M}) \cdot P_{\text{Handoff}_{MF}} \quad (43a)$$

$$\lambda_{MU_M} = \left(1 - N \frac{A_F}{A_M} \right) \cdot \lambda_M \quad (43b)$$

$$\lambda_{MU_FM} = N\lambda_2 \cdot (1 - P_{MU_F}) \cdot P_{\text{Handoff}_{FM}} \quad (43c)$$

$$\lambda_{MU_MM} = (\lambda_{MU_M} + \lambda_{MU_FM} + \lambda_{MU_MM}) \cdot (1 - P_{U_M}) \cdot P_{\text{Handoff}_{MM}}. \quad (43d)$$

REFERENCES

- [1] V. Chandrasekhar, J. G. Andrews, and A. Gatherer, "Femtocell networks: A survey," *IEEE Commun. Mag.*, vol. 46, no. 9, pp. 59–67, Sep. 2008.
- [2] A. Golaup, M. Mustapha, and L. B. Patanapongpibul, "Femtocell access control strategy in UMTS and LTE," *IEEE Commun. Mag.*, vol. 47, no. 9, pp. 117–123, Sep. 2009.
- [3] I. Humar, X. Ge, L. Xiang, M. Jo, and M. Chen, "Rethinking energy-efficiency models of cellular networks with embodied energy," *IEEE Netw. Mag.*, vol. 25, no. 3, pp. 40–49, Mar. 2011.
- [4] Z. Hasan, H. Boostanimehr, and V. K. Bhargava, "Green cellular networks: A survey, some research issues and challenges," *IEEE Commun. Surveys Tuts.*, vol. 13, no. 4, pp. 524–540, Nov. 2011.
- [5] Y. Chen, S. Zhang, S. Xu, and G. Y. Li, "Fundamental trade-offs on green wireless networks," *IEEE Commun. Mag.*, vol. 49, no. 6, pp. 30–37, Jun. 2011.
- [6] Y. Kim, S. Lee, and D. Hong, "Performance analysis of two-tier femtocell networks with outage constraints," *IEEE Trans. Wireless Commun.*, vol. 9, no. 9, pp. 2695–2700, Sep. 2010.
- [7] T. Elkourdi and O. Simeone, "Femtocell as a relay: An outage analysis," *IEEE Trans. Wireless Commun.*, vol. 10, no. 12, pp. 4204–4213, Dec. 2011.
- [8] Y. Zhang, "Resource sharing of completely closed access in femtocell networks," in *Proc. IEEE WCNC*, 2010, pp. 1–5.
- [9] F. Pantisano, M. Bennis, W. Saad, and M. Debbah, "Spectrum leasing as an incentive towards uplink macrocell and femtocell cooperation," *IEEE J. Select. Areas Commun.*, vol. 30, no. 3, pp. 617–630, Apr. 2012.
- [10] W. C. Cheung, T. Q. S. Quek, and M. Kountouris, "Throughput optimization, spectrum allocation, and access control in two-tier femtocell networks," *IEEE J. Select. Areas Commun.*, vol. 30, no. 3, pp. 561–574, Apr. 2012.
- [11] J. Xiang, Y. Zhang, T. Skeie, and L. Xie, "Downlink spectrum sharing for cognitive radio femtocell networks," *IEEE Syst. J.*, vol. 4, no. 4, pp. 524–534, Dec. 2010.

- [12] D. Oh, H. Lee, and Y. Lee, "Power control and beamforming for femtocells in the presence of channel uncertainty," *IEEE Trans. Veh. Technol.*, vol. 60, no. 6, pp. 2545–2554, Jul. 2011.
- [13] V. Chandrasekhar and J. G. Andrews, "Uplink capacity and interference avoidance for two-tier femtocell networks," *IEEE Trans. Wireless Commun.*, vol. 8, no. 7, pp. 3498–3509, Jul. 2009.
- [14] Y. Sun, R. P. Jover, and X. Wang, "Uplink interference mitigation for OFDMA femtocell networks," *IEEE Trans. Wireless Commun.*, vol. 11, no. 2, pp. 614–625, Feb. 2012.
- [15] V. Chandrasekhar, J. G. Andrews, T. Muharemovic, Z. Shen, and A. Gatherer, "Power control in two-tier femtocell networks," *IEEE Trans. Wireless Commun.*, vol. 8, no. 8, pp. 4316–4328, Aug. 2009.
- [16] H. Jo, C. Mun, J. Moon, and J. Yook, "Interference mitigation using uplink power control for two-tier femtocell networks," *IEEE Trans. Wireless Commun.*, vol. 8, no. 10, pp. 4906–4910, Oct. 2009.
- [17] P. Xia, V. Chandrasekhar, and J. G. Andrews, "Open vs. closed access femtocells in the uplink," *IEEE Trans. Wireless Commun.*, vol. 9, no. 12, pp. 3798–3809, Dec. 2010.
- [18] Y. Hou and D. I. Laurenson, "Energy efficiency of high QoS heterogeneous wireless communication network," in *Proc. IEEE VTC Fall*, 2010, pp. 1–5.
- [19] C. Khirallah, J. S. Thompson, and H. Rashvand, "Energy and cost impacts of relay and femtocell deployments in long-term-evolution advanced," *IET Commun.*, vol. 5, no. 18, pp. 2617–2628, Dec. 2011.
- [20] C. Han, T. Harrold, S. Armour, I. Krikidis, S. Videv, P. M. Grant, H. Haas, J. S. Thompson, I. Ku, C.-X. Wang, T. A. Le, M. R. Nakhai, J. Zhang, and L. Hanzo, "Green radio: Radio techniques to enable energy efficient wireless networks," *IEEE Commun. Mag.*, vol. 49, no. 6, pp. 46–54, Jun. 2011.
- [21] K. Zhang, Y. Wang, W. Wang, M. Dohler, and J. Wang, "Energy-efficiency wireless in-home: The need for interference-controlled femtocells," *IEEE Wireless Commun.*, vol. 18, no. 6, pp. 36–44, Dec. 2011.
- [22] F. Cao and Z. Fan, "The tradeoff between energy efficiency and system performance of femtocell deployment," in *Proc. IEEE ISWCS*, 2010, pp. 315–319.
- [23] A. D. Domenico, E. C. Strinati, and A. Duda, "Ghost femtocells: An energy-efficiency radio resource management scheme for two-tier cellular networks," in *Proc. IEEE Eur. Wireless*, 2011, pp. 1–8.
- [24] L. Apio, E. Mino, L. Cucala, O. Moreno, and I. Berberana, "Energy efficiency and performance in mobile networks deployments with femtocells," in *Proc. IEEE PIMRC*, 2011, pp. 107–111.
- [25] I. Ku, C.-X. Wang, and J. S. Thompson, "The spectral, energy and economic efficiency of relay-aided cellular networks," *IET Commun.*, vol. 7, no. 14, pp. 1476–1487, Sep. 2013.
- [26] X. Hong, Y. Jie, C.-X. Wang, J. Shi, and X. Ge, "Energy-spectral efficiency trade-off in virtual MIMO cellular systems," *IEEE J. Sel. Areas Commun.*, vol. 31, no. 10, pp. 2128–2140, Oct. 2013.
- [27] L. Hu and S. Stephen, "Personal communication systems using multiple hierarchical cellular overlays," *IEEE J. Sel. Areas Commun.*, vol. 13, no. 2, pp. 406–415, Feb. 1995.
- [28] S. P. Chung and M. T. Li, "Performance evaluation of hierarchical cellular CDMA networks with soft handoff queueing," *IEEE Trans. Veh. Technol.*, vol. 54, no. 2, pp. 652–672, Mar. 2005.
- [29] L. Kleinrock, *Queueing Systems*. New York, NY, USA: Wiley, 1975.
- [30] G. Mansfield, "Femtocells in the US market—Business drivers and consumer propositions," in *Proc. Femtocells Europe Conf.*, 2008, pp. 1927–1948.
- [31] C. Stuart, "Challenges facing the femtocell market—A realistic view?" in *Proc. 2nd Int. Conf. Home Access Points Femtocells*, Dec. 2007, pp. 1–5.
- [32] [Online]. Available: <http://www.3g.co.uk/PR/July2006/3384.htm>
- [33] C. Bettstetter, H. Hannes, and X. Prez-Costa, "Stochastic properties of the random waypoint mobility model: Epoch length, direction distribution, and cell change rate," in *Proc. 5th ACM Int. Workshop Modeling Anal. Simul. Wireless Mobile Syst.*, 2002, pp. 7–14.
- [34] *IEEE 802.16m Evaluation Methodology Document (EMD)*, IEEE 802.16m08/004r5, Mar. 2009.
- [35] X. Cheng, C.-X. Wang, H. Wang, X. Gao, X.-H. You, D. Yuan, B. Ai, Q. Huo, L. Song, and B. Jiao, "Cooperative MIMO channel modeling and multi-link spatial correlation properties," *IEEE J. Sel. Areas Commun.*, vol. 30, no. 2, pp. 388–396, Feb. 2012.
- [36] X. Ge, K. Huang, C.-X. Wang, X. Hong, and X. Yang, "Capacity analysis of a multi-cell multi-antenna cooperative cellular network with co-channel interference," *IEEE Trans. Wireless Commun.*, vol. 10, no. 10, pp. 3298–3309, Oct. 2011.
- [37] [Online]. Available: <http://www.femtoforum.org/>
- [38] Y. Lin, C. Gan, and C. Liang, "Reducing call routing cost for femtocells," *IEEE Trans. Wireless Commun.*, vol. 9, no. 7, pp. 2302–2309, Jul. 2010.



Xiaohu Ge (M'09–SM'11) received the Ph.D. degree in communication and information engineering from Huazhong University of Science and Technology (HUST), Wuhan, China, in 2003.

He joined HUST in November 2005 and is currently a Professor with the Department of Electronics and Information Engineering. From January 2004 to October 2005, he was a Researcher with Ajou University, Suwon, Korea, and Politecnico Di Torino, Torino, Italy. From June to August 2010, he was a Visiting Researcher with Heriot-Watt University, Edinburgh, U.K. He has published about 70 papers in refereed journals and conference proceedings and has been granted about 15 patents in China. His research interests include mobile communications, traffic modeling in wireless networks, green communications, and interference modeling in wireless communications.

Dr. Ge received the Best Paper Award from the IEEE Global Communications Conference (Globecom 2010). He is leading several projects funded by the National Natural Science Foundation of China (NSFC), China Ministry of Science and Technology (MOST), and industries. He is taking part in several international joint projects, such as the Research Councils UK (RCUK)-funded project UK–China Science Bridges: R and D on (B)4G Wireless Mobile Communications and the EU-FP7-funded project Security, Services, Networking and Performance of Next Generation IP-based Multimedia Wireless Networks. He is currently serving as an Associate Editor for the *Wireless Communications and Mobile Computing Journal* (Wiley), the *International Journal of Communication Systems* (Wiley), *KSII Transactions on Internet and Information Systems*, and the *Journal of Internet Technology*. Since 2005, he has been actively involved in the organization of more than ten international conferences, including serving as the Executive Chair of the 2013 IEEE International Conference on Green Computing and Communications (GreenCom 2013) and as a Technical Program Committee Co-chair of the IEEE 7th International Wireless Internet Conference (WICON 2013). He is a Senior Member of the Chinese Institute of Electronics, a Senior Member of the China Institute of Communications, and a member of the NSFC and China MOST Peer Review College.

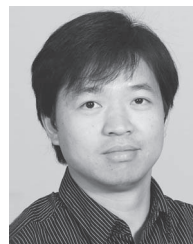


Tao Han (M'13) received the Ph.D. degree in communication and information engineering from Huazhong University of Science and Technology (HUST), Wuhan, China, in 2001.

He is currently an Associate Professor with the Department of Electronics and Information Engineering, HUST. From 2010 to 2011, he was a Visiting Scholar with the University of Florida, Gainesville, FL, USA, as a Courtesy Associate Professor. His research interests include wireless communications, multimedia communications, and

computer networks.

Dr. Han is a Reviewer for the IEEE TRANSACTIONS ON VEHICULAR TECHNOLOGY and other journals.



Yan Zhang (SM'10) received the Ph.D. degree from Nanyang Technological University, Singapore.

Since August 2006, he has been with the Simula Research Laboratory, Fornebu, Norway, where he is currently a Senior Research Scientist. He is an Adjunct Associate Professor with the University of Oslo, Oslo, Norway. His research interests include wireless networks and smart grid communications.

Dr. Zhang is a Regional Editor, an Associate Editor, a Guest Editor, or on the editorial board of a number of international journals.



Guoqiang Mao (SM'08) received the Ph.D. degree in telecommunications engineering from Edith Cowan University, Joondalup, Australia, in 2002.

Between 2002 and 2013, he was an Associate Professor with the School of Electrical and Information Engineering, The University of Sydney, Australia. He is currently a Professor of wireless networking and the Director of the Center for Real-Time Information Networks, University of Technology, Sydney, Ultimo, Australia. He has published more than 100 papers in international conferences and

journals, which have been cited more than 2000 times. His research interests include intelligent transport systems, applied graph theory and its applications in networking, wireless multihop networks, wireless localization techniques, and network performance analysis.

Dr. Mao is the Editor of the *IEEE TRANSACTIONS ON VEHICULAR TECHNOLOGY* and a Co-chair of the IEEE Intelligent Transport Systems Society Technical Committee on Communication Networks.



Cheng-Xiang Wang (S'01–M'05–SM'08) received the B.Sc. and M.Eng. degrees in communication and information systems from Shandong University, Jinan, China, in 1997 and 2000, respectively, and the Ph.D. degree in wireless communications from Aalborg University, Aalborg, Denmark, in 2004.

Since 2005, he has been with Heriot-Watt University, Edinburgh, U.K., where he was first a Lecturer, then a Reader in 2009, and was promoted to Professor in 2011. He is also an Honorary Fellow with the University of Edinburgh, and a Chair/Guest

Professor with Shandong University and Southeast University, Nanjing, China. He was a Research Fellow with the University of Agder, Grimstad, Norway, from 2001 to 2005; a Visiting Researcher with Siemens AG-Mobile Phones, Munich, Germany, in 2004; and a Research Assistant with Technical University of Hamburg-Harburg, Hamburg, Germany, from 2000 to 2001. He has edited one book and published one book chapter and over 180 papers in refereed journals and conference proceedings. His current research interests include wireless channel modeling and simulation, green communications, cognitive radio networks, vehicular communication networks, large multiple-input multiple-output (MIMO), cooperative MIMO, and Beyond-Fourth Generation wireless communications.

Dr. Wang served or is currently serving as an Editor for eight international journals, including the *IEEE TRANSACTIONS ON VEHICULAR TECHNOLOGY* (since 2011) and the *IEEE TRANSACTIONS ON WIRELESS COMMUNICATIONS* (2007–2009). He was the leading Guest Editor for the *IEEE JOURNAL ON SELECTED AREAS IN COMMUNICATIONS* Special Issue on Vehicular Communications and Networks. He served or is serving as a Technical Program Committee (TPC) Member, TPC Chair, and General Chair for over 70 international conferences. He received the Best Paper Awards from the IEEE Global Communications Conference (Globecom 2010), the IEEE International Conference on Communication Technology (ICCT 2011), the International Conference on ITS Telecommunications (ITST 2012), and the IEEE Vehicular Technology Conference (VTC 2013-Fall). He is a Fellow of the Institution of Engineering and Technology (IET), a Fellow of the Higher Education Academy, and a member of the Engineering and Physical Sciences Research Council Peer Review College.



Jing Zhang (M'13) received the M.S. and Ph.D. degrees from Huazhong University of Science and Technology (HUST), Wuhan, China, in 2002 and 2010, respectively.

He is currently an Associate Professor with HUST. He has done research in the areas of multiple-input multiple-output, CoMP, beamforming, and next-generation mobile communications. His current research interests include cellular systems, green communications, channel estimation, and system performance analysis.



Bin Yang received the Bachelor's degree in communication and information system from Huazhong University of Science and Technology, Wuhan, China, in 2012, where he is currently working toward the Doctorate degree.

His research interests include queuing theory, stochastic geometry, and heterogeneous networks.



Sheng Pan received the Bachelor's degree in communication engineering from Hubei University, Baoding, China, in 2012. He is currently working toward the Master's degree with Huazhong University of Science and Technology, Wuhan, China.

His research interests include energy-efficient wireless networks, large-scale antenna systems, and heterogeneous networks.